

Quantitatively scoring behavior from video-recorded, long-lasting fish trajectories



P. Martí-Puig ^{a,*}, M. Serra-Serra ^a, A. Campos-Candela ^{b,c}, R. Reig-Bolano ^a,
A. Manjabacas ^d, M. Palmer ^b

^a Data and Signal Processing Group, U Science Tech, University of Vic - Central University of Catalonia, c/ de la Laura 13, 08500, Vic, Catalonia, Spain

^b Instituto Mediterráneo de Estudios Avanzados, IMEDEA (UIB-CSIC), Miquel Marqués 21, 07190, Esporles, Islas Baleares, Spain

^c Department of Marine Sciences and Applied Biology, University of Alicante, P. O. Box 99, 03080, Alicante, Spain

^d Instituto de Ciencias del Mar, ICM (CSIC), Passeig Martim de la Barceloneta, 37–49, E-08003, Barcelona, Catalonia, Spain

ARTICLE INFO

Article history:

Received 21 February 2017

Received in revised form

13 September 2017

Accepted 10 January 2018

Keywords:

Multi-object tracking
Tracking by identification
Long-lasting tracking
Behavioral assays

ABSTRACT

Scoring animal behavior is increasingly needed for better understanding ecological processes. For example, behavior shapes harvesting likelihood, thus management of harvested resources should improve after accounting for behavior-driven processes. Automatic video-recording at controlled arenas is the most widespread method for scoring behavior. However, long term tracking animals while keeping identity is still an opened challenge. Here, we develop an ad-hoc algorithm for multi-tracking objects during days or even weeks, to fulfill the particular needs for a behavioral assay concerning a fish species targeted by recreational fishing. Specifically, we overcome the challenge of keeping fish identity in a context where they often disappeared from the camera when entering a shelter, the pixel size was low compared to the size of the arena and the lighting was constrained by the wellbeing of the fish. This work may contribute to better assess the behavioral features of fish in long-lasting lab conditions.

© 2018 Elsevier Ltd. All rights reserved.

1. Introduction

Animals in wild populations are continuously at risk of being predated or harvested but some individuals have larger survival likelihood than others. For example, it is well known that hunting and fishing implies size-related selection (Matsumura et al. (2011); Uusi-Heikkilä et al. (2015)). Behavior-related selection has been reported as well (Biro and Sampson (2015); Ciuti et al. (2012); Diaz Pauli et al. (2015); Härkönen et al. (2016); Jørgensen and Holt (2013); Madden and Whiteside (2014)), so certain behavioral phenotypes are selected against (Alós et al. (2012), (2015); Diaz Pauli et al. (2015); Klefth et al. (2013); Vainikka et al. (2016)). When the traits under selection are genetically heritable, the population may be driven to a harvest induced evolution (de Roos et al. (2006); Law (2007); (Philipp et al., 2015); Uusi-Heikkilä et al. (2015)), which implies a number of unintended and undesired outcomes that ultimately reduce yield (Matsumura et al. (2011); Mollet et al. (2016)).

However, such negative outcomes on population dynamics are

expected only when selection gradients are consistent in time, that is, when a specific animal exhibits a given personality (i.e., it tends to behave in a similar way). The concept of animal personality (Dingemanse and Wolf (2010), (2013); Mittelbach et al. (2014)) is based in two patterns. First, the existence of between-individual differences in behavior that are consistently repeated at the long term (i.e., behavioral types) is often recognizable over the within-individual variability. Second, several behavioral traits are often correlated, shaping what it has been named as behavioral syndromes (Sih et al. (2004)), thus animal personality can be scored after knowing how the animal uses space in a number of contexts. Technological improvements have led to the widespread use of underwater devices for data collection, continuous monitoring and estimates of population parameters in the field (Williams et al. (2010); Aguzzi et al. (2013)). Indeed, cabled video observatories for the remote, long-term and high-frequency monitoring of fish and their environment have been used in coastal temperate areas (Aguzzi et al. (2013), (2015); Matabos et al. (2014)) to study behavioural response to environmental changes or human perturbations (Mecho et al. (2017)). Some studies in the field by using camera devices (e.g., (Alós et al. (2015); Mecho et al. (2017))) have already focused on the role of the behaviour in processes of

* Corresponding author.

E-mail address: pere.marti@uvic.cat (P. Martí-Puig).

artificial selection. Nevertheless, the study of behavioural types (or personality traits) by video recording in the field is still an open challenge since recognition at the individual level is required. Therefore, the actual limitation for a more widespread implementation of behavior focused management is seemingly not conceptual but technical: fish personality can be scored from their patterns of space use but only after a long-lasting observation time which includes individual fish recognition. In that context, video-recording fish in experimental conditions (i.e., tanks) is becoming a widespread method (Laskowski et al. (2016); Ozbilgin and Glass (2004); Papadakis et al. (2012)), in spite that some potential drawbacks (e.g., extrapolating the results to field conditions; (Niemelä and Dingemanse (2014); Závorka et al. (2015))). Alongside, unsupervised tracking on video-recorded is also increasingly required to better quantify long-term behavioral patterns, which in turn would allow scoring individuals in terms of animal personality. Hence, real-time tracking of video images should be preferred because rigorous statistical analysis of the behavioral patterns associated with movement involve not only long-lasting experiments but also unsupervised extraction of a number of space-use metrics (Papadakis et al. (2012)).

Unsupervised tracking of moving targets over a video sequence has been addressed from different fields (Burghardt et al. (2004); Dankert et al. (2009); de Chaumont et al. (2012); Kabra et al. (2012); Kühl and Burghardt (2013) and Trucco and Plakas (2006)). Even concerning the specific case of fish tracking, several techniques have been proposed (Delcourt et al. (2013); Dell et al. (2014) for a review), enabling advances in behavioral studies. However, some challenges remain concerning long-lasting precise and accurate tracking of animals, especially when the experimental settings do not fit high standards. On one hand, how to preserve individuals identities throughout long time periods remains an opened question (Delcourt et al. (2013), but see Noldus et al. (2001) and Straw and Dickinson (2009)); on the other, specific experimental settings usually impose additional difficulties (e.g., arenas with uniform, white and artificial light conditions are generally used (Delcourt et al. (2006))).

Most tracking algorithms uses Kalman filters or particle filters for predicting positions of moving targets (Kalman et al. (1960); Nummiaro et al. (2003); Pinkiewicz et al. (2008)). Target detection is mainly based on detecting shape, color or finding blobs, which may be achieved via histograms analysis or attempting to maximize correlations between statistical models (Sattar and Dudek (2006)). Further, detection and tracking stages can be combined together in order to remove faulty detections (Fontaine et al. (2008); Spampinato et al. (2008); Xia et al. (2016); Pérez-Escudero et al. (2014); Chuang and Hwang (2016)). Recently, methods based on deep learning have been popularized. For example, the features of the fish head have been used to identify targets along frames (XU et al. (2017)). Similarly, (Qian et al. (2014)) combined Kalman filtering with the determinant of Hesssian. As deep learning methods have reveled as efficient alternatives for recognizing visual patterns, convolutional neural networks (CNN) has been implemented also (XU et al. (2017)). For instance, (Wang et al. (2016)) combined CNN with head fish identification, being able to track several individuals at the same time.

However, actual applications of these methods require highly standardized settings in terms of, for example, a well lightened and small scenario. This is not the case of the experiments that are currently conducted for assessing the links between behavior and vulnerability to fishing of a small-bodied marine fish (Alós et al. (2013)). This species, *Serranus scriba*, is one of the main targets of the recreational angler from Mallorca (Western Mediterranean) (Alós et al. (2013)). In this case, the experimental settings were particularly challenging. Individuals can appear and disappear from

the scene because they were allowed to spend long periods of time in a shelter. However, fish identity must be preserved along days, which have been achieved by tagging the fish with colored marks. Provided that fish were submitted to several behavioral experiments, the tank must be continuously monitored during all the day-light period. Moreover, the experimental arena was very large in comparison to the sizes of colored tags, which imposed to deal with high resolution images in order to represent tags with enough number of pixels. Finally, the lightening conditions of the scenario must emulate those experienced by the fish at wild conditions; thus light had a strong blue component that difficult to discriminate fish from background and distorts colors. In addition, the lightening setting produces reflections and it was not uniform.

Even under those unfavorable experimental settings, we developed and described an ad-hoc algorithm for remote, long-term unsupervised-tracking of a number of fish moving in a tank. Moreover, the tracking algorithm has been coupled with proper statistical tools for extracting a number of metrics related with space use from fish trajectories, which will be used for analyzing of fish behavior and scoring fish personality.

2. Materials and methods

2.1. Model species

Serranus scriba is a simultaneous hermaphrodite serranid, widely distributed in the Mediterranean Sea. It is heavily exploited by the local recreational angling fishery (Alós et al. (2013)), which preferentially captures individuals with low reproductive investment and high adult body size (Alós et al. (2014)). Further, evidences of behavioural-related selection on exploration rates has been reported (Alós et al. (2012)).

2.2. Capture and tagging procedure

Fish were obtained from the wild by angling in coastal waters (from 5 up to 10 m depth) near the research experimental station (LIMIA), in Andratx Bay, on the SW coast of Mallorca, where experiments were conducted. Fish were double tagged with T-tags painted in different fluorescent colours (white (0), red (R) and green (G) tags were combined in pairs). Tagging was done by means of a hollow-needle tagging-gun according to (Dell (1968)). Length and weight measures were taken at the same time. Manipulation time did not exceed 1 min. Overall, transport, tagging and release into tank procedure took about 30 min. No mortality was observed neither during this procedure, nor during the experiment.

The experiments were conducted with adult fish (total body length 15.7 ± 1.9 cm; mean mass 53 ± 21.5 g; mean \pm standard deviation). Fish were distributed in groups of 5 individuals of approximately the same size (0.6 individuals/ m^2). Temperature water was the same as that of the sea (26.2 ± 0.6 C; mean \pm 1 standard deviation over all days of trials).

2.3. Scenario and experiment description

2.3.1. Scenario

The experimental tank, with dimensions $4\text{ m} \times 2\text{ m}$ (length \times width) and 30 cm water depth, was filled with sea-water and fitted with an open circuit filtering system. Due to the evidences that the behavioral performance of fish may be affected by environmental light conditions (e.g. Marchesan et al. (2005); Berdahl et al. (2013)); the experimental tank was illuminated emulating the natural light conditions of the habitat of the species, and at the same time covering the requirement of an homogeneous illumination in all the extension of the tank. The experimental light atmosphere was

provided by a light system (LED strip lights) with three-modes on/off switching that automatically let the transition from 6500 K white daylight to 460 nm blue sunset light to darkness. A diurnal-nocturnal sequence of illumination was projected onto the water (i.e., a day: night light cycle). Specifically, diurnal conditions ranged from 7am to 7pm (white light was switched on an hour after the blue one and was switched off an hour before to ensure a progressive illumination of the tank with conditions similar to the sunrise and sunset ones); and the darkness conditions ranged from 7pm to 7am. The experimental tank was divided in two areas: the shelter (1 m long) and the arena (3 m long). Shelter was done with stone blocks and artificial plastic plants to provide a safe area for the fish (Fig. 1). To ensure fish were not disturbed during the experiment and to avoid changes in the illumination conditions that could affect the quality or recordings, the tank was isolated from the rest of the laboratory with black curtains, avoiding in that way changes in illumination or reflexes in the surface of the water from abroad; and minimizing visual stimulus or other unintended stimulus. Cameras and lights were controlled remotely, out of sight of the experimental arena.

2.3.2. Camera and electronic equipment

An Axis P1428-E IP camera captures the arena images from a zenithal position (nearly 2 m above the water surface) and send them to a computer in order to be processed. The Axis P1428-E camera is compact and outdoor-ready providing up to 8.3 MP/4K HD of resolution at 30 frames per second. To achieve real-time requirements the camera works at 10 frames per second. The computer has a Intel®.i7 CPU with 6 cores and 12 threads, 32 GB of RAM and 2 TB of hard disk. The software, developed in python 3.5 using OpenCV 3.0, runs on Ubuntu 16.04 OS. That machine has also a Matlab® 2016a license to perform post-processing tasks. The time required to process an image is always less than 90ms. The system is configured to process ten images per second.

2.3.3. Experiment description

The general objective was to describe the trajectories and the space use of every fish within groups of a maximum of 5 individuals. Fish were identified with a combination of one or two red (R) or green (G) tags, according the combinations: R, RR, RG, G, GG (Fig. 2). A given fish group remained in the tank for one or two weeks. During such a time, fish were submitted to several behavioral test every day. Behavioral tests are fully detailed elsewhere (Campos-Candela et al., in prep). However, provided that the objective of this paper is to demonstrate the usefulness of the general strategy, here we focused in a single behavioral test. Exploration test are aimed to describe the space use when a new item is located at the center of the arena ([Walsh and Cummins \(1976\)](#); [Adriaenssens and Johnsson \(2013\)](#)). One exploration test was completed daily between 8:30am to 10:30am. Here we focused in the first four exploration tests experienced by a given fish group.

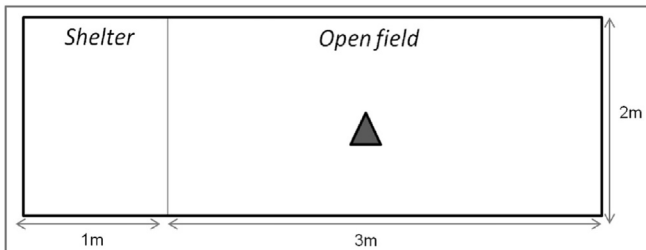


Fig. 1. Design of the experimental tank where behavioural tests were carried on.

2.4. Multi-tracking algorithm

Let us consider an incoming color image $\mathbf{I}_n(x, y)$, (x and y indexes pixel positions and n frames) which is pre-processed time-to-time in order to detect and identify fishes by means of tag colors. $\mathbf{I}_n(x, y)$ is composed by their red, green and blue components $\mathbf{R}_n(x, y)$, $\mathbf{G}_n(x, y)$ and $\mathbf{B}_n(x, y)$ as $\mathbf{I}_n(x, y) = (\mathbf{R}_n(x, y), \mathbf{G}_n(x, y), \mathbf{B}_n(x, y))$, although to simplify notation x and y are omitted to get $\mathbf{I}_n = (\mathbf{R}_n, \mathbf{G}_n, \mathbf{B}_n)$.

2.4.1. Detection

In the RGB color space red and green colors are directly identified from \mathbf{R}_n and \mathbf{G}_n components. The first step consists on the subtraction of the remaining background red and green components which in small proportions are present in the water from the original image. The result is multiplied by a factor 1.8 as it is shown:

$$\mathbf{R}_n \leftarrow 1.8(\mathbf{R}_n - r_n \mathbf{O}) \quad (1)$$

$$\mathbf{G}_n \leftarrow 1.8(\mathbf{G}_n - g_n \mathbf{O}) \quad (2)$$

\mathbf{O} stands for the all-ones matrix and r_n and g_n are measures of the red and green background levels. Values r_n and g_n are computed every frame in order to follow possible variations of lighting. Such values are obtained by computing the mean of all points inside a sub-image which is large enough to average the effect of a tag inside it in the moment of the update. The factor 1.8 have been obtained empirically and it depends on the lighting. Proceeding in this way the pixels from red and green tags will reach levels near saturation. That operation will simplify color detection further down.

Then, \mathbf{R}_n , \mathbf{G}_n , \mathbf{B}_n components are used to compute two of the three HSV color space components: \mathbf{H}_n and \mathbf{V}_n , while \mathbf{S}_n is not required because the modification performed in \mathbf{R}_n and \mathbf{G}_n by 1 and 2 makes detection independent of saturation and very few dependent of \mathbf{V}_n .

\mathbf{H}_n and \mathbf{V}_n are used to construct \mathbf{BR}_n and \mathbf{BG}_n binary images from which the red and green objects will be detected respectively. The HSV color space is closed to the way in which humans perceive color. In HSV, hue (H) represents color which are clearly defined according human perception, value (V) is the brightness of the color and saturation (S) indicates the range of grey in the color space. Considering that \mathbf{H}_n and \mathbf{V}_n take values in the range 0–1, \mathbf{BR}_n and \mathbf{BG}_n matrices are obtained by applying the next conditions to their pixels according to:

$$\mathbf{BR}_n = ((\mathbf{H}_n < 0.0894) \text{ or } (\mathbf{H}_n > 0.7821)) \text{ and } (\mathbf{V}_n > 0.38) \quad (3)$$

and

$$\mathbf{BG}_n = (\mathbf{H}_n > 0.1117) \text{ and } (\mathbf{H}_n < 0.5028) \text{ and } (\mathbf{V}_n > 0.38) \quad (4)$$

Then, \mathbf{BR}_n and \mathbf{BG}_n present groups of connected pixels of value 1 concentrated in the small regions where red and green tags (if any) appear, respectively. \mathbf{BR}_n and \mathbf{BG}_n provide the area of interest (ROI) in the original image. The pixel positions of those small connected regions identify red and green tags from the background (0s). By identifying those regions and computing their center of masses and areas (in number of pixels) the specimens present in each image are precisely located.

However, previously to characterize tags, two major issues must be attended. The first; due to structural constrains in the emplacement of lights, some reflections appear inevitably in the scenario and there is not a perfect uniform lighting in all the area. The strategy of dynamically adapt the red and green components presented in 1, 2 fights against non uniform lighting, but light

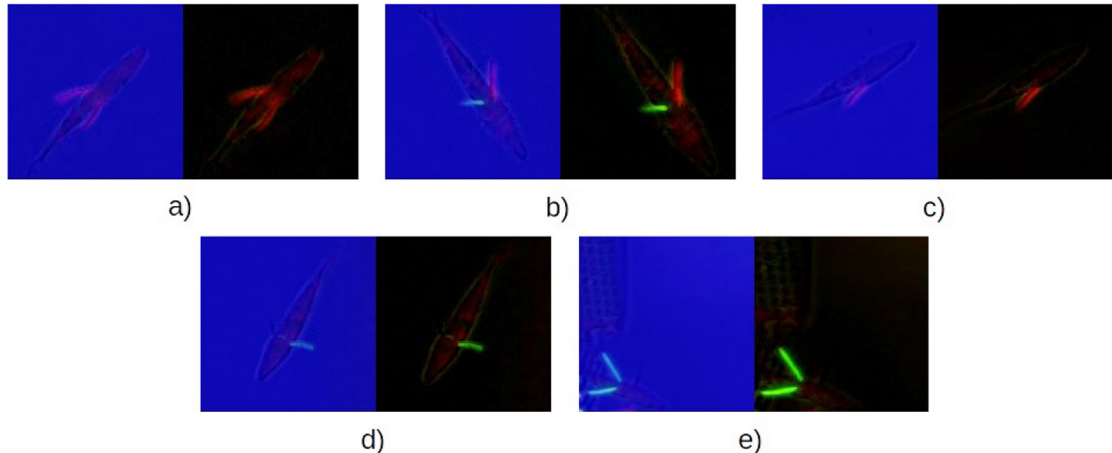


Fig. 2. Specimens with color tags. On the left, the specimen captured in the scene. On the right, the same images after applying equations (1) and (2) and without the blue component. Specimens are tagged as: a) RR b) RG c) R d) G and e) GG.

reflections contain some red and green components that causes false object detection. The simplest way to combat it is by eliminating those regions with a mask \mathbf{M} . That mask is obtained by detecting the areas where reflections are produced, and applying a morphological *dilation* to be sure of capturing reflections when they move for the presence of small waves in the water surface. That causes the lose of tags in the moment that fishes crosses the zone of reflections in the similar way that tags are lost when they suffer an occlusion. The second; the operations described in 3 and 4 occasionally split a single tag in more than one region. So, previously to count regions and computing sizes and centers, a morphological *closing* must be done in order that disconnected closed regions will be reconnected. That operation is performed by a square of 5×5 pixels as structuring element (SE). The *closing* is obtained by applying the *dilation* of \mathbf{BR}_n (and \mathbf{BG}_n) by SE, followed by the *erosion* of the outcome by the same SE. The size of SE will depend on the imatge resolution and the size of tags.

Then, for each frame n , centroids of red and green detected objects are stored in \mathbf{Cr}_n and \mathbf{Cg}_n lists ordered by their areas in descending order. Areas are also stored in \mathbf{ar}_n and \mathbf{ag}_n lists. \mathbf{Cr}_n and \mathbf{Cg}_n are lists of points of different lengths containing their x , y coordinates and their frame number. If no detection of red color is produced in frame n then corresponding \mathbf{Cr}_n and \mathbf{ar}_n remain empty. In order to introduce the notation used, lets suppose that in frame-number 256 there was observed three red regions; then \mathbf{Cr}_{256} could take the form shown in 5 and the information stored inside can be addressed as it is shown in 6:

$$\mathbf{Cr}_{256} = \begin{pmatrix} x_1 & y_1 & 256 \\ x_2 & y_2 & 256 \\ x_3 & y_3 & 256 \end{pmatrix} \quad (5)$$

$$\mathbf{Cr}_{256}(2) = [x_2 \ y_2 \ 256] ; \mathbf{Cr}_{256}(2)(1 : 2) = [x_2 \ y_2] \quad (6)$$

Note that we only need \mathbf{Cr}_n , \mathbf{Cg}_n , \mathbf{ar}_n and \mathbf{ag}_n to register the whole experiment. This data are obtained and stored in real-time. From these data the tracks can be obtained by applying different strategies that can be executed not necessarily in real-time. In this way any algorithmic improvement can always be tested again.

2.4.2. Early identification and post-processing stage

Theoretically, according section 2.3, only four tags of the same color are significant to identify the five possible specimens in the scene, however there are considered a maximum of 5 objects of the

same color in order to deal with possible classification errors. That step is done once per frame and do not require analyzing past results. For every frame n , the early classification takes information from \mathbf{Cr}_n , \mathbf{Cg}_n , \mathbf{ar}_n and \mathbf{ag}_n as inputs and computes the lists of positions $\mathbf{p_RR}_n$, $\mathbf{p_R}_n$, $\mathbf{p_RG}_n$, $\mathbf{p_GG}_n$, $\mathbf{p_G}_n$ by taking information of colors and analyzing distances of centroids. As multiple assignment errors can appear caused by detection mistakes, in that first classification we admit the possibility of obtaining more than one individual identified as having same tag. That occurs, for instance, if in one frame there are detected more than one R because individual RR or RG present in the scene are bad detected. A post-processing step will correct those isolated cases. However, if in frame n there is no presence of a particular specimen, its corresponding list remains empty. *Early identification* pseudo-code is provided in algorithm 3 in which constants $A_B = 250$ and $A_S = 5$ are empirically assigned as they are dependent on the scene, the camera resolution and the size of tags. A_B is used to control cases where double tags of the same color are merged to form a bigger one and A_S controls some noise introduced occasionally in by light reflections. Basic red and green tag identification and early fish identification strongly compacts information required for tracking specimens as we replace a high resolution image by the few values stored in the those lists. Those list of few elements per frame avoid to transfer and store several Terabytes of 4K-high-resolution images (videos) as they contain the required information to track specimens in the post-processing stage. As pointed before, although almost tags are properly detected, natural movements of fishes, light reflections, etc. cause that composed tags (RR, RG and GG) are occasionally bad identified. For instance, in the set of RR tags drawing a sequential continuous path one miss-classified R appears. In that particular case in frame n , $\mathbf{p_R}_n$ will has more than one value if the real R tag is also present. That is the reason because lists can contain more than one element. That supposes a big inconsistency that can be corrected. We can consider re-labeling or simply removing the point. As in the post-processing stage there is no important time restrictions we have considered the reallocation by applying logical criteria and computing space-time distances. After applying those algorithms $\mathbf{p_RR}_n$, $\mathbf{p_R}_n$, $\mathbf{p_RG}_n$, $\mathbf{p_GG}_n$ and $\mathbf{p_G}_n$ have a maximum of one element in position n , otherwise they are empty. Fig. 3 shows the simplified sequence of operations of the early identification stage in a block diagram. The following sequence of operations, which we call the post-processing stage, can be performed indistinctly in real time, because they are computationally very efficient, or not. The post-processing stage will allow future algorithm

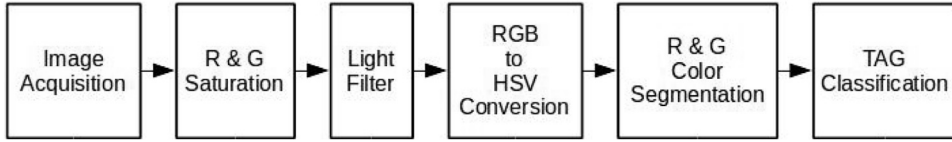


Fig. 3. Block diagram showing the sequence of operations of the early detection stage.

improvements and it is mainly based on Kalman filtering, which is explained in next section. The results of the early identification stage are shown in Fig. 4 a for a time-sequence of 500 frames. Then, in the post-processing stage, a linear Kalman filter is used to obtain positions and instant velocities, as well as to estimate state variables when measures are not available due to occlusions or failures in tag segmentation. Fig. 4 b shows, for the same sequence of 500 frames, the track coordinates obtained after applying the Kalman filter. Those tracks are represented in figure ?

2.4.3. The Kalman filter

According to the state space linear model:

$$\mathbf{x}_n = \mathbf{A}\mathbf{x}_{n-1} + \mathbf{w}_n \quad (7)$$

where vector $\mathbf{x}_n = [x_{\text{X}}, y_{\text{V}}]^T$ is the state variable at instant n and (x, y) and (v_x, v_y) define position and velocity components of a given specimen, respectively. \mathbf{A} is the state transition matrix:

Algorithm 1: Early classification

```

Data: Crn, Cgn, arn, agn
Result: p_RRn, p_Rn, p_RGn, p_GGn, p_Gn
begin
    lr ← length(arn); lg ← length(agn); nr ← 0; ng ← 0; fish ← []
    for i ← 1 to lr do
        Crn(i)(3) ← 0
        if arn(i) > AB then
            fish.append ← Crn(i); fish.append ← Crn(i)
            nr ← nr + 2
        else if arn(i) > AS and arn(i) ≤ AB then
            fish.append ← Crn(i)
            nr ← nr + 1
    for i ← 1 to lg do
        Cgn(i)(3) ← 0
        if agn(i) > AB then
            fish.append ← Cgn(i); fish.append ← Cgn(i)
            ng ← ng + 2
        else if agn(i) > AS and agn(i) ≤ AB then
            fish.append ← Cgn(i)
            ng ← ng + 1
    nT ← nr + ng
    if nT == 1 then
        if nR == 1 then
            | p_Rn.append ← fish(1,1:2)
        else
            | p_Gn.append ← fish(1,1:2)
    else
        nF, n ← size(fish)
        for e ← 1 to nF do
            for a ← e to nF do
                d ← distance(fish(e,1:2),fish(a,1:2))
                if d < 30 and fish(e,3)=0 and e ≠ a then
                    if e < nr and a ≤ nr then
                        | p_RRn.append ← 0.5(fish(e,1:2))+fish(a,1:2))
                        | fish(e,3) ← 1; fish(a,3) ← 1
                    else if e ≤ nr and a > nr then
                        | p_RGn.append ← 0.5(fish(e,1:2))+fish(a,1:2))
                        | fish(e,3) ← 1; fish(a,3) ← 1
                    else if e > nr and e < nT and a ≤ nT and a > nr + 1 then
                        | p_GGn.append ← 0.5(fish(e,1:2))+fish(a,1:2))
                        | fish(e,3) ← 1; fish(a,3) ← 1
                    else if ((e==a and d==0) or d ≥ 30) and fish(e,3)==0 then
                        if e > nr and a == nT then
                            | p_Gn.append ← fish(e,1:2)
                            | fish(e,3) ← 1
                        else if e ≤ nr and a == nT then
                            | p_Rn.append ← fish(e,1:2)
                            | fish(e,3) ← 1
*/ 0: is not read */
*/ R */
*/ G */
*/ RR */
*/ RG */
*/ GG */
*/ G */
*/ R */

```

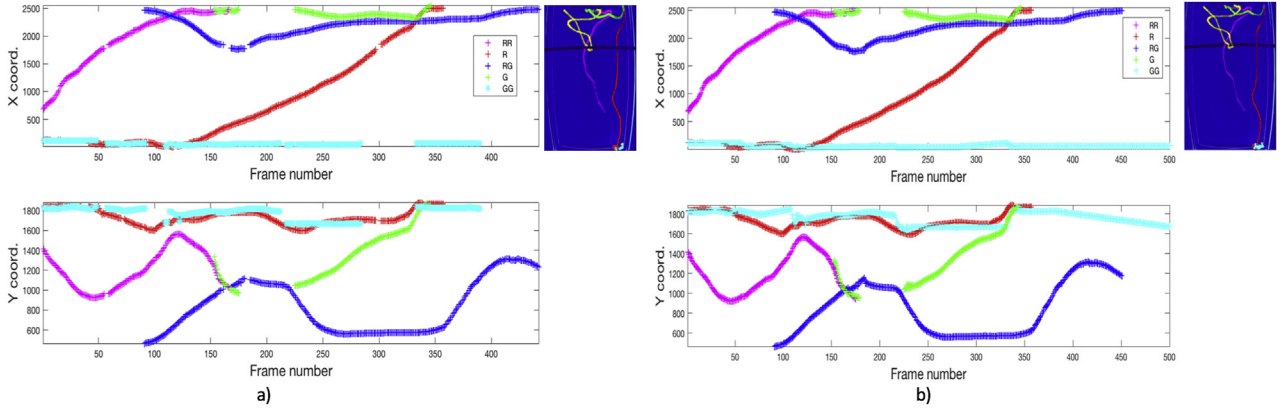


Fig. 4. a) The x and y coordinates after the TAG Classification operation performed on a time-sequence of 500 frames for five specimens b) The x and y coordinates after applying the Kalman filter (for the same sequence of 500 frames).

$$\mathbf{A} = \begin{bmatrix} 1 & \Delta_t & 0 & 0 \\ 0 & 1 & 0 & 0 \\ 0 & 0 & 1 & \Delta_t \\ 0 & 0 & 0 & 1 \end{bmatrix}, \quad (8)$$

and \mathbf{w}_n the process noise vector which is assumed to follow a zero mean normal multivariate distribution with covariance \mathbf{Q}_n ($\mathbf{w}_n \approx N(0, \mathbf{Q}_n)$).

The measurement equation takes the form:

$$\mathbf{z}_n = \mathbf{Hx}_n + \mathbf{v}_n, \quad (9)$$

being \mathbf{z}_n the vector of measures (i.e. when dealing with RR specimen $\mathbf{z}_n = \mathbf{p}_n \mathbf{RR}_n^T$), \mathbf{v}_n the vector of measurement noise for which it is also assumed a zero mean normal distribution with covariance \mathbf{R}_n ($\mathbf{v}_n \approx N(0, \mathbf{R}_n)$). \mathbf{H} , the state-to-measurement matrix, takes the form:

$$\mathbf{H} = \begin{bmatrix} 1 & 0 & 0 & 0 \\ 0 & 0 & 1 & 0 \end{bmatrix} \quad (10)$$

Under normal operating conditions when the pre-processing step provides \mathbf{z}_n for frame n , the recursive Kalman filter is defined by the well-known four steps. Considering \mathbf{P}_n the error covariance, the first step is devoted to predict state $\hat{\mathbf{x}}_n^-$ and error covariance as follows:

$$\hat{\mathbf{x}}_n^- = \mathbf{Ax}_{n-1} \quad (11)$$

$$\mathbf{P}_n^- = \mathbf{AP}_{n-1}\mathbf{A}^T + \mathbf{Q} \quad (12)$$

Note that symbols $\hat{\cdot}$ and $\bar{\cdot}$ indicate *estimation* and *prediction*, respectively. Then \mathbf{P}_n^- is used to compute the Kalman gain \mathbf{K}_n as:

$$\mathbf{K}_n = \mathbf{P}_n^- \mathbf{H}^T \left(\mathbf{H} \mathbf{P}_n^- \mathbf{H}^T + \mathbf{R} \right)^{-1} \quad (13)$$

The state is estimated by weighting through \mathbf{K}_n the prediction and the measure according to:

$$\hat{\mathbf{x}}_n = \hat{\mathbf{x}}_n^- + \mathbf{K}_n (\mathbf{z}_n - \mathbf{H} \hat{\mathbf{x}}_n^-) \quad (14)$$

Finally, last step computes the error covariance:

$$\mathbf{P}_n = \mathbf{P}_n^- - \mathbf{K}_n \mathbf{H} \mathbf{P}_n^- \quad (15)$$

and the algorithm is prepared to next iteration. In the case where no measures are available the estimation of the estate is performed

directly by the prediction part according the model described in 7. The same is performed in the case in which the distance between the predicted value and the measure is greater than a value C_p (given in pixels) impossible to be covered by a fish in 0.1 s. The velocity v_x and v_y components are obtained directly by the Kalman observations by returning the complete state variable. Every time the fish enters in the shelter, the filter status is reset and each new track fragment starts with the parameters by default. From v_x and v_y we obtain the modulus of the instant velocity.

2.5. Scoring behavior from trajectories

Crude fish trajectories were not readily usable for comparing fish behavior. Instead, to describe general patterns of activity and exploration, six metrics were derived. First, phi was the proportion of time spent active (i.e., outside the shelter). Second, preliminary histograms of the fish position along the longitudinal axis of the tank (Fig. 1), strongly suggest that fish tend to spend more time either near the shore or near the wall opposite to the shore, while spending short time at the middle of the arena. According to such a bimodal use of space, the data was fitted to an ad-hoc distribution consisting in the mixture of two (negative) exponential distributions, with respectively the origins at the shelter and at the opposite wall. This distribution is described by three parameters: p (proportion of time spent near the shelter, being $1-p$ the proportion of the time spent near the opposite wall), $\lambda_{shelter}$ (the rate of the exponential distribution when the fish is near the shelter) and λ_{opp} (the rate of the exponential distribution when the fish is near the opposite wall). Third, d_{total} was the total distance traveled during 2 h measured as the sum of all between-frame displacements. Finally, preliminary histograms of the fish velocity. Displacements between consecutive frames strongly suggest that empirical speed distribution may be adjusted to a (negative) exponential distribution, which was described by λ_{speed} (the rate of the exponential distribution). The three exponential rates were inversed (1/rate) in order to facilitate interpretation of the parameter in terms of average. Empirical data was fitted to the distributions (either the ad-hoc distribution for positions along the longitudinal axis of the tank or the exponential distribution for speed) using a Bayesian fitting procedure. Raw data was reduced in order to alleviate temporal autocorrelation (1000 evenly distributed points in the temporal series were selected). Model, data and initial values were prepared using the R package (<https://www.r-project.org/>) from where a MCMC iterator was call (Jags; <http://mcmc-jags.sourceforge.net/>). In all the cases, uninformative, flat priors were used and convergence was checked using conventional

criteria, after appropriate burning and thinning. Posterior distributions were estimated from three independent MCMCs (1000 valid iterations each). The remaining parameters (d_{total} and ϕ) were computed directly from the trajectories using an R ad-hoc script.

3. Results

The experimental setting has demonstrated to be able to successfully video recording the tank during all the experiment duration. The multi-tracking algorithm has been tested in four behavioral test of 2 h each in order to validate the strategy. Three fishes tagged as RR, RG and R were continuously tracked during each of this four tests. The estimated tracks for each specimen were verified by checking the coherence of transitions between the arena and the shelter and by visual inspection. Kalman filters in the post-processing stage help to fill missing points and contributes to clean tracks. Furthermore, the state model used also provides estimations of x , y instantaneous velocity components. Fig. 5 a shows the time-sequences of x and y coordinates and the modulus of the instant velocity for one specimen in an entire experiment while 5.b shows the representation of those tracks in the arena. The trajectories of the three fish considered in one of the 2-h long test is shown in Fig. 6. The multi-tracking algorithm has successfully used to reconstruct the trajectory of the fish even when moving in a group, as suggested by the examples displayed at Fig. 6.

3.1. An overview of the activity patterns detected

Concerning the behavioral pattern depicted by the trajectories, the general patterns and the between- and within-fish variability of the six parameters distilled from the trajectories are shown in Fig. 7. In spite that the results refers only to three fish and four 2-h trajectories per day, some general patterns can be suggested. For instance, the individual #17 was the individual that spent less time out the shelter but when it is outside the shelter, it spent more time near the shelter and with an average position closer to it. It also showed the highest average speed. Overall, this metrics seems to suggest a conservative, low risk behavior. Opposite, the individual #3 (in blue at Fig. 7) spent more time out the shelter and father

away. Despite showing less average speed than red and similar to green, it was the one that travelled more distance, so it explored a larger area during the four days.

4. Conclusions

The experimental setting has demonstrated to be able to successfully video record the tank during all the experiment duration. Furthermore, in order to deal with the experimental constrains and avoid storing huge amount of video sequences, we present an ad-hoc approach performed in two steps. The first step is done in real-time, and detects and transfers frame-to-frame object positions and other characteristics (as their areas) towards a computer. The information extracted in this step is required to identify the tags and hugely compacts high resolution video images (4K) processed at a rate of 10 frames per second into a smallest set of values. In long-lasting experiments that will be the information preserved and stored. The second step consists on processing that information

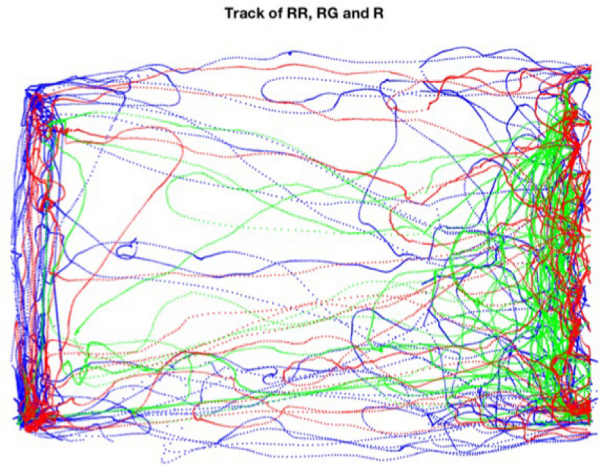


Fig. 6. Track representation of an entire experiment of about 2 h. There are three fishes tagged as RR, R and RG.

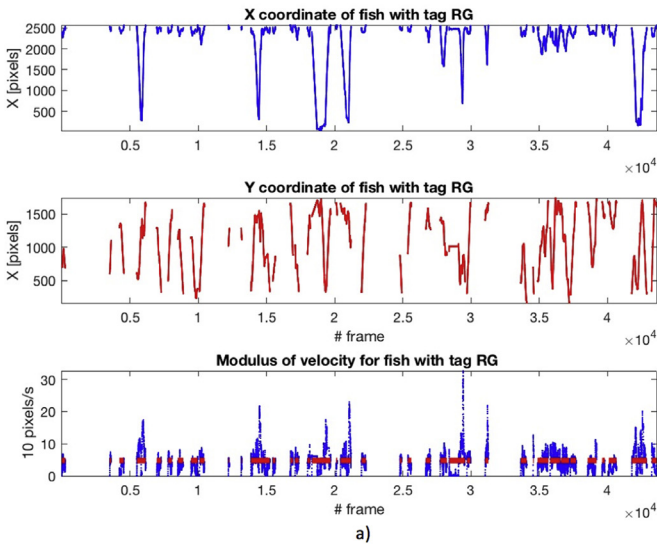
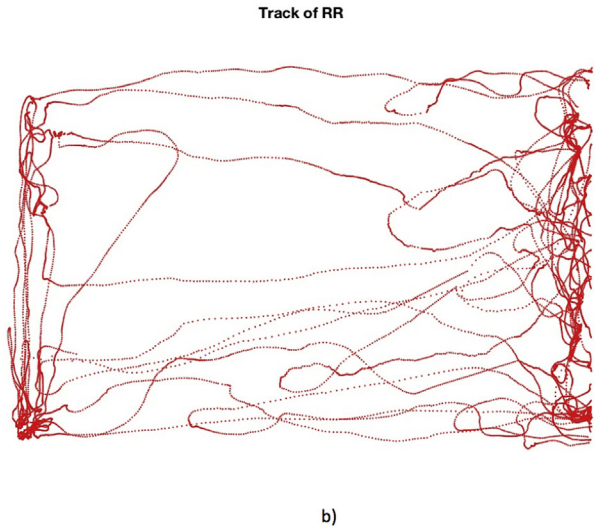


Fig. 5. a) On the top, time-series of x coordinates (longitudinal magnitude) registered for an individual tagged as RG along a complete experiment. Level above 2500 represents the shelter entrance in which the specimens disappear. In the middle time-series of y coordinates. At the bottom time-series of the modulus of the instant velocity. b) Track representation.



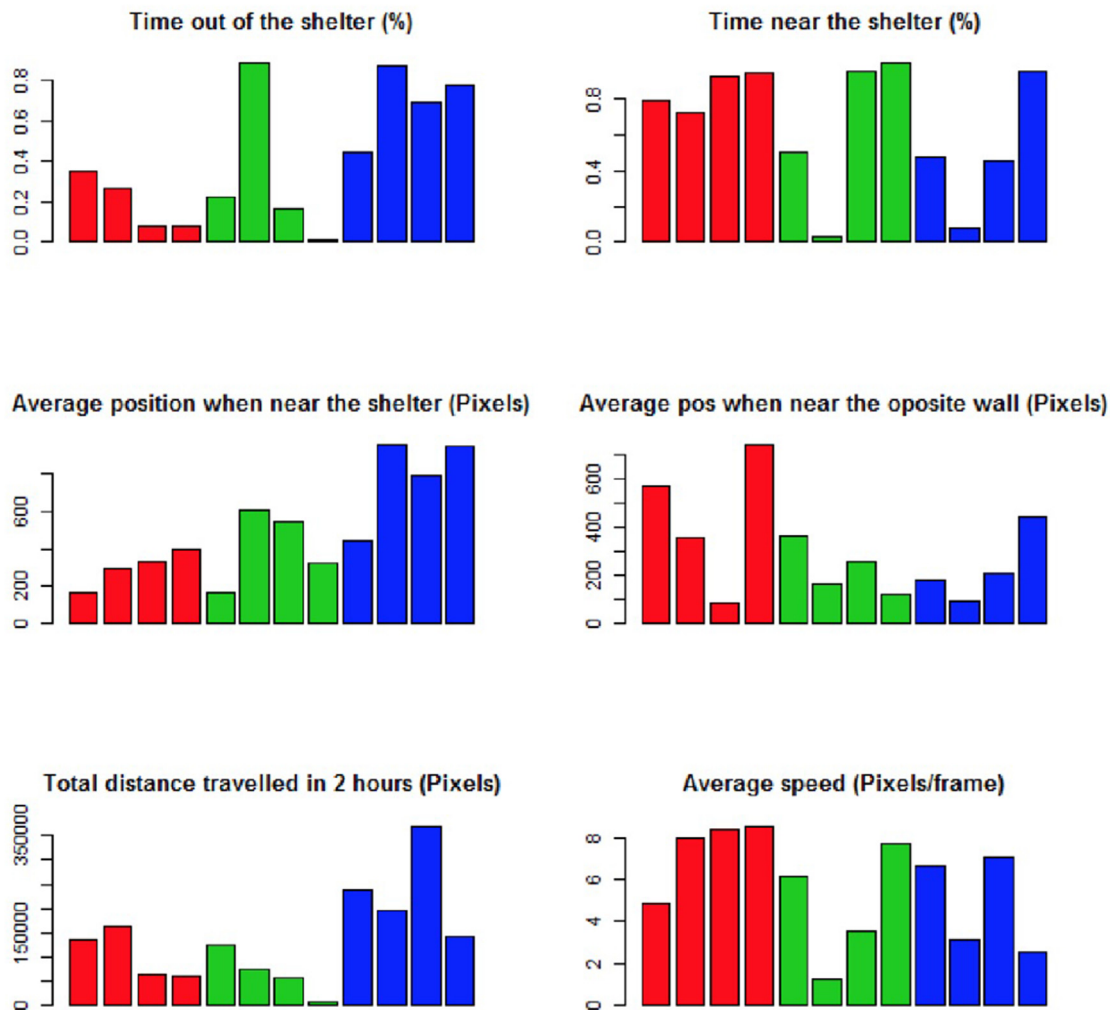


Fig. 7. Individual values for the six metrics calculated to measure exploration and activity patterns. Results for three fish are presented here. Each color correspond to an individual and each column correspond to each experimental day (or temporal replicate).

to obtain the final tracks. It must not necessarily be done in real time. Moreover, we propose up to six metric for scoring fishes from trajectories, based in the use of shelter, the distribution fish position in relation to the shelter, the total distance traveled and the average speed. The preliminary results presented here are a successful proof of concept that the combination of video recording, and long-lasting trajectory reconstruction can be used for scoring fish behavior, and contribute to better understand the behavioral features of fish from long-lasting experiments. A better understanding of individual behavioural patterns in experimental conditions may help to understand better the observed behavioural patterns in the field (e.g., in comparative studies between areas with different conditions) and to figure out what could be the role of behaviour in artificial selection contexts.

Ethics

Animal care and all experimental procedures were authorized by those responsible for the Ethics Committee for Animal Experimentation of the University of the Balearic Islands (CEEA-UIB), through a permit (ref. CEEA/60/0916) to the FENOFISH Project (ref. CTM2015-69126-C2-1-R) funded by the Spanish Ministry of Science and Competitiveness; and were carried out in strict accordance

with the recommendations from Directive 2010/175/UE, adhering to 176 Spanish law (RD53/2013, BOE n. 34 February 8th 2013). Our study did not involve endangered or protected species. All efforts were made to minimize fish handling and harm.

Acknowledgments

This work has been partially supported by the Spanish Government projects PHENOFISH with references: CTM2015-69126-C2-1-R and CTM2015-69126-2-R, and is a contribution of the Joint Research Unit IMEDEA-LIMIA. A.C.C. was supported by a FPU predoctoral fellowship (ref.FPU13/01440) from the Spanish Ministry of Education, Culture and Sports (MECD). The authors thank José Antonio Antonio García del Arco, from ICM (CSIC), for his help in the selection of the IP camera.

References

- Adriaenssens, B., Johnsson, J.I., 2013. Natural selection, plasticity and the emergence of a behavioural syndrome in the wild. *Ecol. Lett.* 16 (1), 47–55.
- Aguzzi, J., Costa, C., Company, J., Fujihara, Y., Favali, P., Tunnicliffe, V., Matabos, M., Canals, M., Menesatti, P., 2013. The new synthesis of cabled observatory science: technology meets deep-sea ecology. In: Underwater Technology Symposium (UT), 2013 IEEE International. IEEE, pp. 1–8.
- Aguzzi, J., Doya, C., Tecchio, S., Leo, De, F. C., Azzurro, E., Costa, C., Sbragaglia, V., Del

- Río, J., Navarro, J., Ruhl, H.A., Company, J.B., Favali, P., Purser, A., Thomsen, L., Catalán, I.A., Sep 2015. Coastal observatories for monitoring of fish behaviour and their responses to environmental changes. *Rev. Fish Biol. Fish.* 25 (3), 463–483. <https://doi.org/10.1007/s11160-015-9387-9>.
- Alós, J., Alonso-Fernández, A., Catalán, I.A., Palmer, M., Lowerre-Barbieri, S., 2013. Reproductive output traits of the simultaneous hermaphrodite *Serranus scriba* in the western Mediterranean. *Sci. Mar.* 77 (2), 331–340.
- Alós, J., Palmer, M., Arlinghaus, R., 2012. Consistent selection towards low activity phenotypes when catchability depends on encounters among human predators and fish. *PLoS One* 7 (10), e48030.
- Alós, J., Palmer, M., Catalán, I.A., Alonso-Fernández, A., Basterretxea, G., Jordi, A., Buttay, L., Morales-Nin, B., Arlinghaus, R., 2014. Selective exploitation of spatially structured coastal fish populations by recreational anglers may lead to evolutionary downsizing of adults. *Mar. Ecol. Prog. Ser.* 503, 219–233.
- Alós, J., Palmer, M., Trías, P., Díaz-Gil, C., Arlinghaus, R., 2015. Recreational angling intensity correlates with alteration of vulnerability to fishing in a carnivorous coastal fish species. *Can. J. Fish. Aquat. Sci.* 72 (October 2014), 217–225.
- Berdahl, A., Torney, C.J., Ioannou, C.C., Faria, J.J., Couzin, I.D., 2013. Emergent sensing of complex environments by mobile animal groups. *Science* 339 (6119), 574–576.
- Biro, P.A., Sampson, P., 2015. Fishing directly selects on growth rate via behaviour: implications of growth-selection that is independent of size. *Proceedings of the Royal Society B* 282 (1802), 13–15.
- Burghardt, T., Calic, J., Thomas, B., 2004. Tracking Animals in Wildlife Videos Using Face Detection. *Ewimt.*
- Chuang, M., Hwang, J.W., 2016. A feature learning and object recognition framework for underwater fish images. *IEEE Trans. Image Process.* 25 (4), 1862–1872.
- Ciuti, S., Muhly, T.B., Paton, D.G., McDevitt, A.D., Musiani, M., Boyce, M.S., 2012. Human selection of elk behavioural traits in a landscape of fear. *Proc. Biol. Sci.* 279, 4407–4416.
- Dankert, H., Wang, L., Hoopfer, E.D., Anderson, D.J., Perona, P., 2009. Automated monitoring and analysis of social behavior in *Drosophila*. *Br. J. Pharmacol.* 6 (4), 297–303.
- de Chaumont, F., Coura, R.D.-S., Serreau, P., Cressant, A., Chabout, J., Granon, S., Olivo-Marin, J.-C., mar 2012. Computerized video analysis of social interactions in mice. *Br. J. Pharmacol.* 9 (4), 410–417.
- de Roos, A.M., Boukal, D.S., Persson, L., 2006. Evolutionary regime shifts in age and size at maturation of exploited fish stocks. *Proc. Biol. Sci.* 273 (1596), 1873–1880.
- Delcourt, J., Becco, C., Yliffe, M.Y., Caps, H., Vandewalle, N., Poncin, P., 2006. Comparing the EthoVision 2.3 system and a new computerized multitracking prototype system to measure the swimming behavior in fry fish. *Behav. Res. Meth.* 38 (4), 704–710.
- Delcourt, J., Denoël, M., Yliffe, M., Poncin, P., 2013. Video multitracking of fish behaviour: a synthesis and future perspectives. *Fish Fish.* 14, 186–204.
- Dell, A.I., Bender, J.A., Branson, K., Couzin, I.D., de Polavieja, G.G., Noldus, L.P.J.J., Pérez-Escudero, A., Perona, P., Straw, A.D., Wikelski, M., Brose, U., 2014. Automated image-based tracking and its application in ecology. *Trends Ecol. Evol.* 29, 417–428.
- Dell, M.B., 1968. A new fish tag and rapid, cartridge-fed applicator. *Trans. Am. Fish. Soc.* 97 (1), 57–59.
- Diaz Pauli, B., Wiech, M., Heino, M., Utne-Palm, A.C., 2015. Opposite selection on behavioural types by active and passive fishing gears in a simulated guppy *Poecilia reticulata* fishery. *J. Fish. Biol.* 86 (3), 1030–1045.
- Dingemanse, N.J., Wolf, M., 2010. Recent models for adaptive personality differences: a review. *Phil. Trans. Biol. Sci.* 365, 3947–3958.
- Dingemanse, N.J., Wolf, M., 2013. Between-individual differences in behavioural plasticity within populations: causes and consequences. *Anim. Behav.* 85 (5), 1031–1039.
- Fontaine, E., Lentink, D., Kranenburg, S., Müller, U.K., van Leeuwen, J.L., Barr, A.H., Burdick, J.W., 2008. Automated visual tracking for studying the ontogeny of zebrafish swimming. *J. Exp. Biol.* 211 (8), 1305–1316.
- Härkönen, L., Hyvärinen, P., Niemelä, P.T., Vainikka, A., 2016. Behavioural variation in Eurasian perch populations with respect to relative catchability. *Acta Ethol.* 19 (1), 21–31.
- Jorgensen, C., Holt, R.E., 2013. Natural mortality: its ecology, how it shapes fish life histories, and why it may be increased by fishing. *J. Sea Res.* 75, 8–18. <https://doi.org/10.1016/j.seares.2012.04.003>.
- Kabra, M., Robie, A.A., Rivera-Alba, M., Branson, S., Branson, K., 2012. JAABA: interactive machine learning for automatic annotation of animal behavior. *Br. J. Pharmacol.* 10 (1), 64–67.
- Kalman, R.E., et al., 1960. A new approach to linear filtering and prediction problems. *J. Basic Eng.* 82 (1), 35–45.
- Klefthof, T., Pieterk, T., Arlinghaus, R., 2013. Impacts of domestication on angling vulnerability of common carp, *Cyprinus carpio*: the role of learning, foraging behaviour and food preferences. *Fish. Manag. Ecol.* 20 (2–3), 174–186.
- Kühl, H.S., Burghardt, T., 2013. Animal biometrics: quantifying and detecting phenotypic appearance. *Trends Ecol. Evol.* 28 (7), 432–441.
- Laskowski, K.L., Monk, C.T., Polverino, G., Alós, J., Nakayama, S., Staaks, G., Mehner, T., Arlinghaus, R., 2016. Behaviour in a standardized assay, but not metabolic or growth rate, predicts behavioural variation in an adult aquatic top predator *Esox lucius* in the wild. *J. Fish. Biol.* 88 (4), 1544–1563.
- Law, R., 2007. Fisheries-induced evolution: present status and future directions. *Mar. Ecol.: Prog. Ser.* 335, 271–277.
- Madden, J.R., Whiteside, M.A., 2014. Selection on behavioural traits during ‘unselective’ harvesting means that shy pheasants better survive a hunting season. *Anim. Behav.* 87, 129–135.
- Marchesan, M., Spoto, M., Verginella, L., Ferrero, E.A., 2005. Behavioural effects of artificial light on fish species of commercial interest. *Fish. Res.* 73 (1–2), 171–185.
- Matabos, M., Bui, A.O., Mihály, S., Aguzzi, J., Juniper, S.K., Ajayamohan, R., 2014. High-frequency study of epibenthic megafaunal community dynamics in barkley canyon: a multi-disciplinary approach using the neptune Canada network. *J. Mar. Syst.* 130, 56–68.
- Matsumura, S., Arlinghaus, R., Dieckmann, U., 2011. Assessing evolutionary consequences of size-selective recreational fishing on multiple life-history traits, with an application to northern pike (*Esox lucius*). *Evol. Ecol.* 25 (3), 711–735.
- Mecho, A., Aguzzi, J., De Mol, B., Lastras, G., Ramirez-Llodra, E., Bahamon, N., Canals, M., et al., 2017. Visual faunistic exploration of geomorphological human-impacted deep-sea areas of the north-western mediterranean sea. *J. Mar. Biol. Assoc. U. K.* 1–12.
- Mittelbach, G.G., Ballew, N.G., Kjelvik, M.K., Fraser, D., 2014. Fish behavioral types and their ecological consequences. *Can. J. Fish. Aquat. Sci.* 71 (6), 927–944.
- Mollet, F.M., Poos, J.J., Dieckmann, U., Rijnsdorp, A.D., 2016. Evolutionary impact assessment of the North Sea plaice fishery. *Can. J. Fish. Aquat. Sci.* 73 (November 2015), 1126–1137.
- Niemelä, P.T., Dingemanse, N.J., 2014. Artificial environments and the study of adaptive personalities. *Trends Ecol. Evol.* 29 (5), 245–247.
- Noldus, L.P., Spink, A.J., Tegelenbosch, R.A., 2001. EthoVision: a versatile video tracking system for automation of behavioral experiments. *Behav. Res. Meth. Instrum. Comput.* : J. Polyn. Soc. 33 (3), 398–414.
- Nummiaro, K., Koller-Meier, E., Van Gool, L., jan 2003. An adaptive color-based particle filter. *Image Vis Comput.* 21 (1), 99–110.
- Ozbilgin, H., Glass, C., 2004. Role of learning in mesh penetration behaviour of haddock (*Melanogrammus aeglefinus*). *ICES (Int. Counc. Explor. Sea) J. Mar. Sci.* 61, 1190–1194.
- Papadakis, V.M., Papadakis, I.E., Lamprianidou, F., Glaropoulos, A., Kentouri, M., 2012. A computer-vision system and methodology for the analysis of fish behavior. *Aquacult. Eng.* 46, 53–59.
- Pérez-Escudero, A., Vicente-Page, J., Hinz, R.C., Arganda, S., de Polavieja, G.G., 2014. idTracker: tracking individuals in a group by automatic identification of unmarked animals. *Br. J. Pharmacol.* 11 (7), 743–748.
- Philipp, D.P., Claussen, J.E., Koppelman, J.B., Stein, J.A., Cooke, S.J., Suski, C.D., Wahl, D.H., Sutter, D.A.H., Arlinghaus, R., 2015. Fisheries-induced evolution in largemouth bass: linking vulnerability to angling, parental care, and fitness. *Black Bass Divers. Multidiscip.Sci. Conserv.* 82, 223–234.
- Pinkiewicz, T., Williams, R., Purser, J., 2008. Application of the particle filter to tracking of fish in aquaculture research. In: *Proceedings - Digital Image Computing: Techniques and Applications, DICTA 2008*. IEEE, pp. 457–464.
- Qian, Z., Cheng, X., Chen, Y., 2014. Automatically detect and track multiple fish swimming in shallow water with frequent occlusion. *PLoS One* 9 (9), e106506.
- Sattar, J., Dudek, G., 2006. On the performance of color tracking algorithms for underwater robots under varying lighting and visibility. *IEEE Int. Conf. Robot. Autom.* 2006, 3550–3555.
- Sih, A., Bell, A., Johnson, J., 2004. Behavioral syndromes: an ecological and evolutionary overview. *Trends Ecol. Evol.* 19 (7), 372–378.
- Spampinato, C., Chen-Burger, Y.-H., Nadarajan, G., Fisher, R.B., 2008. Detecting, tracking and counting fish in low quality unconstrained underwater videos. *Image Process.* 514–519.
- Straw, A.D., Dickinson, M.H., 2009. Motmot, an open-source toolkit for realtime video acquisition and analysis. *Source Code Biol. Med.* 4, 5.
- Trucco, E., Plakas, K., 2006. Video Tracking: a Concise Survey.
- Uusi-Heikkilä, S., Whiteley, A.R., Kuparinen, A., Matsumura, S., Venturelli, P.A., Wolter, C., Slatte, J., Primmer, C.R., Meinelt, T., Killen, S.S., Bierbach, D., Polverino, G., Ludwig, A., Arlinghaus, R., 2015. The evolutionary legacy of size-selective harvesting extends from genes to populations. *Evol. Appl.* 8 (6), 597–620.
- Vainikka, A., Tammela, I., Hyvärinen, P., 2016. Does boldness explain vulnerability to angling in Eurasian perch *Perca fluviatilis*. *Cur. Zool.* 62 (2), 109–115.
- Walsh, R.N., Cummins, R.A., 1976. The Open-Field Test: a critical review. *Psychol. Bull.* 83 (3), 482–504.
- Wang, S.H., Zhao, J.W., Chen, Y.Q., 2016. Robust tracking of fish schools using CNN for head identification. *Multimed. Tool. Appl.* 1–19.
- Williams, K., Rooper, C.N., Towler, R., 2010. Use of stereo camera systems for assessment of rockfish abundance in untrawlable areas and for recording pollock behavior during midwater trawls. *Fish. Bull.* 108 (3), 352–362.
- Xia, C., Chon, T.S., Liu, Y., Chi, J., Lee, J.M., 2016. Posture tracking of multiple individual fish for behavioral monitoring with visual sensors. *Ecol. Inf.* 36, 190–198.
- Xu, Z., Cheng, X.E., feb 2017. Zebrafish tracking using convolutional neural networks. *Sci. Rep.* 7, 42815. <http://www.nature.com/articles/srep42815>.
- Závorka, L., Aldvén, D., Näslund, J., Höjesjö, J., Johnsson, J.I., 2015. Linking lab activity with growth and movement in the wild: explaining pace-of-life in a trout stream. *Behav. Ecol.* 00, 1–8.